공학석사 학위논문

비색계 센서로서 은 나노입자의 *in-situ* 합성으로 유도된 카르복시메틸 셀룰로오스 금속겔에 관한 연구

Study on carboxymethyl cellulose metallogel induced by
in-situ synthesis of silver nanoparticles as colorimetric sensors

2019 년 8 월

서울대학교 대학원
융합과학부 나노융합전공
송 유 진

Abstract

Study on carboxymethyl cellulose metallogel induced by *in-situ* synthesis of silver nanoparticles as colorimetric sensors

Yujin Song

Program in Nano Science and Technology

Graduate School of Convergence Science and Technology

Seoul National University

A novel colorimetric sensing platform based on CMC-AgNPs metallogel was proposed to monitor the temperature history and quality of perishable products stored at low temperature. The CMC metallogel, fabricated in the presence of Ag+, incorporates ionic crosslinking of biopolymers, complexation between reactants, and subsequent *in-situ* synthesis of AgNPs, which are designed to lead the color of metallogel from colorless to dark brown depending on temperature and time. The metallogels and AgNPs with the material were observed by

rheology, XRD, and FT-IR. Color changes associated with temperature, time, and metal ion precursors were examined by UV-visible spectroscopy and colorimetry.

The longer the exposure time to abuse temperatures such as room temperature (25 ℃) or high temperature (60 ℃), the deeper the color of metallogel. The CMC-AgNPs metallogel-based sensing platform can be used as a colorimetric sensor that provides cost-effective, safe, and reliable information that indirectly records the temperature history of the product as well as a new strategy to evaluate the quality of perishable products related to time-temperature history without complicated equipment.

Table of Contents

List of Figures

Chapter 1. Introduction

1.1.   Motivation

Perishable products such as food, vaccines, and medicines can be easily damaged over time due to pathogen contamination and/or various external factor. Above all, the temperature is the most influential factor affecting the quality of these products. As chilled/refrigerated distributed products are mostly heat-sensitive, maintaining high-quality requires that a process monitor and control the appropriate temperature during distribution and storage [1, 2]. The freshness of these products is often directly linked to safety. In order to maintain freshness, it is important to maintain proper storage temperature and to manage expiration date. The intake of the right food with the right freshness makes the body healthy, but in the opposite case, eating food and getting sick. According to data from the Centers for Disease Control and Prevention (CDC), 48 million people suffer from foodborne illness each year, with 128,000 hospitalizations and about 3,000 deaths in the United States. However, the quality of many products has been assessed by inaccurate values called "shelf life", which assumes that the product is stored at a constant temperature range, without any consideration of external factors [3]. Indeed, since products can be exposed to a variety of temperature fluctuations in the supply chain from manufacturing to the consumer, they can become deteriorated or decayed owing to the influence of external factors such as humidity, circumstance, and temperature,

even if the shelf life has not passed [4]. It is proposed as a significant issue for public health. Eventually, temperature monitoring systems such as time-temperature indicators or integrators (TTIs), which predict the quality based on the time-temperature history undergone by the product, have been extensively researched in recent years.

Foodborne agents	Estimated annual number of illnesses		Estimated annual number of hospitalizations		Estimated annual number of deaths	
	Number (90% credible interval)	%	Number (90% credible interval)	%	Number (90% credible interval)	%
31 known pathogens	9.4 million (6.6–12.7 million)	20	55,961 (39,534–75,741)	44	1,351 (712–2,268)	44
Unspecified agents	38.4 million (19.8–61.2 million)	80	71,878 (9,924–157,340)	56	1,686 (369–3,338)	56
Total	47.8 million (28.7–71.1 million)	100	127,839 (62,529–215,562)	100	3,037 (1,492–4,983)	100

Figure 1. The estimated annual number of domestically acquired, foodborne illnesses, hospitalizations, and deaths through food, in the United States [5].

Eventually, to address this issue, temperature monitoring systems such as time-temperature indicators or integrators (TTIs), which predict the quality based on the time-temperature history undergone by the product, have been extensively researched in recent years [6, 7].

1.2.   Time-temperature indicator

TTI (Time Temperature Indicator) is a label attached to a package that indicates the time-temperature history of food during distribution and storage. These indicators have used an indirect way of predicting and representing the freshness of products according to the color changing with time-temperature history. The practical shelf life of a perishable product such as food, vaccine, and blood is determined by various factors such as gas composition, humidity, and temperature. Among various storage factors, the temperature is the most influential factor for food degradation. Thus, TTI is a technology that provides a simple means to manage the food supply pathways and enables the safety and quality of perishable products throughout their entire life spans from their manufacturing to consumption by end-users. Since the color and other physical properties of TTIs vary as a function of time, it provides the actual grade of the freshness of the product in which the TTI is used by showing the color, contrast, or any other variable visible characteristic. Various basic requirements of TTIs are to be able to effectively express continuous, irreversible changes in temperature change. Also, it should be non-toxic, cost-effective and sensitive to temperature changes. Currently, the price of TTI is about 1-20 cents, which has sufficient competitiveness.
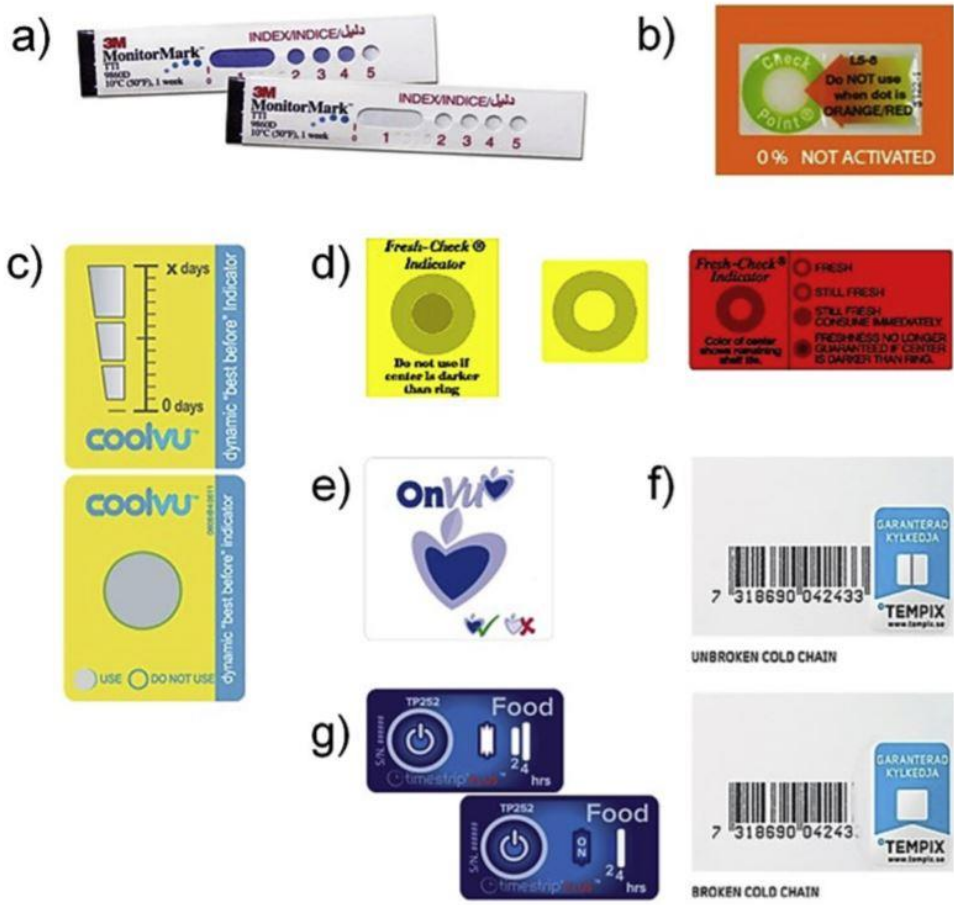
Figure 2. Time-temperature indicator labels [8].

TTIs have categorized based on electronics, physicochemical, and nanomaterials-based mechanism. Electronics-based TTIs are often integrated with data loggers, and radio frequency identification (RFID) tags, enabling accurate and easy-to-read [9]. However, they are complex and expensive to use for consumers. TTIs based on physicochemical principles induced by enzymatic reactions [10], polymerization [11], and diffusions [12] are limited in

that they are costly and lacks uniformity making it challenging to track the overall temperature history for products [13]. TTIs derived from unique properties of nanomaterials are relatively cost-effective and simple, apply in the field immediately, and are promptly available to consumers [6]. Several kinds of nanomaterials-TTIs have been reported as alternatives to conventional sensors by complementing the limitations of above that. Recently as the development progresses, these fields have been actively studied for practical implementation.

1.3. Food nanotechnology

Nanotechnology has emerged in various scientific and technological fields, besides TTIs, related to the inherent characteristics that characteristics such as optical [14], mechanical [15], magnetic [16], and electrical properties [17] distinct from the bulk materials. In spite of many advantages, the question of sustainable applications continues to be posed by the toxicity and environmental effects of nanoparticles. Current trends in nanomaterials research are integrated with hydrogels or green chemistry to overcome limitations associated with risk of human health and environment.
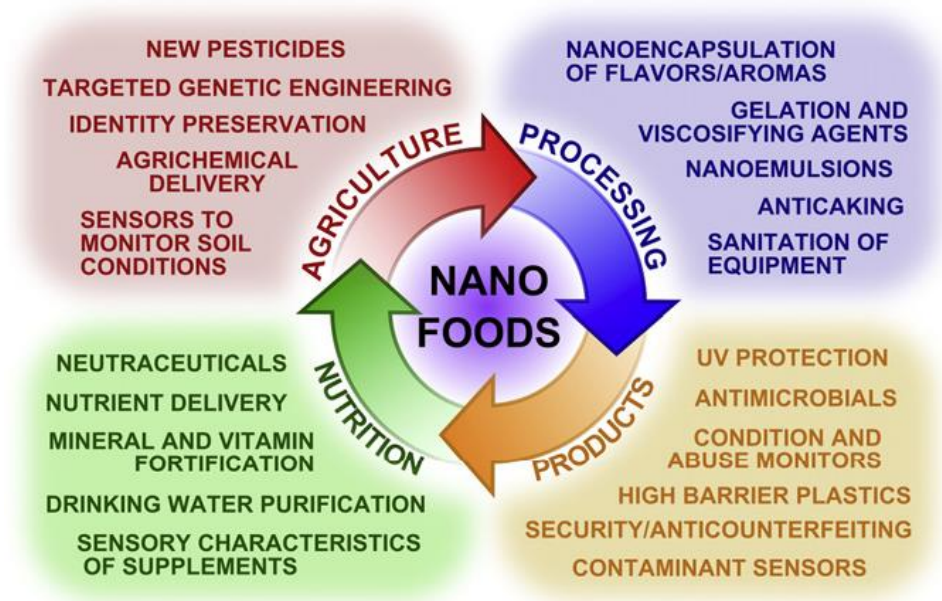
Figure 3. Applications of nanotechnology in food [18].

In particular, metallogel which incorporated metal into the biopolymer gel network not only represents properties of nanoparticles and gels but also acts as a constrained template for *in-situ* synthesis of metal nanoparticles including gold and silver [19]. Plasmonic nanoparticles embedded in metallogel exhibit the localized surface plasmon resonance (LSPR), which can display various bright colors. Furthermore, changes in their size and shape lead to a slight shift of the LSPR band and as a consequence, development in the color expression of the nanoparticles. These type of gels have contributed to increased sensitivity in optical, chemical sensor, biosensor, and colorimetric sensor using these specific characteristics of LSPR [20, 21]. Notwithstanding their significant optical properties, there are only a few reports that

investigate the potential of metallogels as colorimetric sensors.

In this study, CMC-AgNPs metallogel was introduced as a colorimetric sensor to monitor the temperature. CMC, a derivative of cellulose, is a biocompatible and biodegradable biopolymer widely used for medical materials such as tissue generation and drug delivery [22]. The anionic group at the polymer chain can significantly coordinate to a metal cation with high electron affinity. AgNPs have more sharp surface plasmon resonance peak than other metal nanoparticles [23]. In particular, the exclusive optical properties of AgNPs play a vital role in several biomedical application and sensor. Notably, our experiment indicates that CMC tends to react with silver precursors ($AgNO_3$) to form metallogels. The AgNPs *in-situ* synthesized in a metallogel lead to a distinguishable color signal from yellow to brown by SRP change with a particle size corresponding to time and temperature. The result confirmed that CMC-AgNPs metallogels are accompanied by visual changes with time and temperature, which is an indicator of the time-temperature history experienced by the product. To the best our knowledge, this is a novel colorimetric sensor that is inexpensive, user-friendly, portable, reliable, and suitable for large scale production to determine the quality of perishable products based on CMC-AgNPs metallogel.

14

Chapter 2. Experiment

2.1. Materials

Sodium carboxymethyl cellulose (Na-CMC) was purchased from Junsei Chemical Co.,

Ltd. (Japan). Copper (II) chloride anhydrous (CuCl$_2$) and Iron (III) chloride hexahydrate

(FeCl$_3 \cdot 6H_2O$) was supplied by Samchun Pure Chemical (Korea). Silver nitrate (AgNO$_3$, 0.1M)

and gold chloride (III) trihydrate (HAuCl$_4 \cdot 3H_2O$) was purchased from Sigma-Aldrich Co.

(USA). All chemical reagents used as received without any further purification and all

procedures used millipore water (> 18 MΩ cm) obtained from a Barnstead EASYpure Ⅱ

system unless otherwise noted.

2.2. Preparation of CMC-AgNPs metallogels

For the preparation of CMC-AgNPs metallogels as colorimetric sensors, Na-CMC

solution (1 mg/ml) was prepared by dissolving its powder in deionized water at room

temperature (RT). AgNO$_3$ solution (0.1 M) was added into the CMC solution at 0, 20 and 30%

(v/v) respectively, under stirring at RT to synthesize *in-situ* silver nanoparticles (AgNPs)

embedded in metallogels. The color transition of the metallogels was observed with naked-eye from colorless to dark brown.

2.3. Characterization

The absorption spectrum of AgNPs embedded in metallogels was measured on a UV-vis microplate reader (Bio-Tek Synergy H1, USA). The size and morphology of synthesized nanoparticles were imaged using a high-resolution transmission electron microscope (HR-TEM, JEM-3010-JEOL, 300 kV). To prepare the HR-TEM sample, generally, a few drop of CMC-AgNPs solution was located on 400 mesh carbon-coated TEM formvar/copper grid, and excess solution was blotted off by using filter paper. The grid was then wholly dried at room temperature for more than 6h. The crystalline structure of the synthesized AgNPs was confirmed using XRD (Rigaku Smartlab diffractometer) equipped in the diffraction angle range $2\theta = 10\text{-}80°$ with Cu- Kα radiation ($\lambda = 0.154184$ nm). Fourier transform infrared spectrometer (FTIR) was used to probe functional groups changes in CMC. Transmission spectra were recorded on a Bruker VERTEX 70 series FTIR spectrophotometer (Bruker optics, Germany). All measurement was performed in the range 400-4000 cm-1 at a 4 cm-1 resolution.

The rheological behavior of CMC-AgNPs metallogels was investigated by operating

parallel plate rheometer (ARES, Advanced Rheometric Expansion System). Samples were

loaded with a 50 mm parallel plate geometry at 25 ℃. Typical rheometer gap was about 1-2

mm. Dynamic time sweep experiment was carried out at a frequency of 1 rad/s, 20% strain at

25 ℃ to observe the storage and loss modulus values (respectively G´ and G˝).

2.4. Colorimetric sensing of CMC-AgNPs metallogels

The color measurements of CMC metallogels was measured using a colorimeter (CM-5,

Konica Minolta, Japan) according to CIE L*, a*, b* values (L*: lightness, a*: redness, and b*:

yellowness). The total color differences (ΔE) were determined as follows (Liu and Yang 2013):

$\Delta E = [(\Delta L^*)^2 + (\Delta a^*)2 + (\Delta b^*)^2]^{1/2}$

where $\Delta L^*, \Delta a^*, \Delta b^*$ is the lightness from black to white, redness from red to green, and

yellowness form yellow to blue difference between value of initial time and each time interval,

respectively.

Chapter 3. Results and discussion

3.1. Biopolymer-metal nanoparticle metallogels

As is well known, -COOH and -OH groups located in the polymer backbone are useful components for green synthesis of metal nanoparticles by reducing metal ions [22]. Herein, a colorimetric sensor was developed to record the temperature history of frozen products through CMC metallogel incorporating AgNPs inside the polymer matrix. The CMC-AgNPs metallogels formed with the silver atom as gelators serve as an *in-situ* synthesis template for AgNPs and the particles are stabilized by -COOH and -OH groups. A schematic diagram of the formation process of the CMC-AgNPs metallogel used in our study is shown in Fig. 4. Our approach assumes that the higher the temperature, the faster the AgNPs embedded in metallogels grow, followed by changing color from light yellow to dark brown. Heating leads to generate larger particles by merging the smaller ones and induce more nucleation. At this time, the visible colorimetric change occurs due to the size of particles, so that the temperature history can be readily detected.
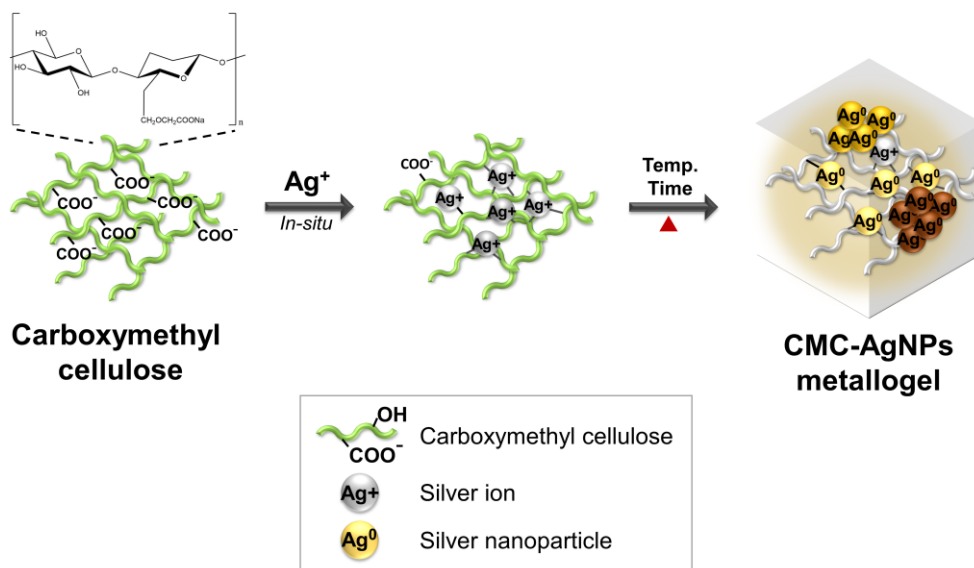
Figure 2. A schematic representation of CMC-AgNPs metallogel formation.

The biopolymers both CMC and alginate, which are known to be abundant in carboxylic groups and hydroxyl groups, were used for the selection of polymers for the fabrication of colorimetric metallogels. The color development and sol-gel transition were observed by adding 0, 20, 25, and 30 v/v (%) silver nitrate solution into 1 mg/ml CMC and alginate solutions, respectively (Fig. 5). The reaction between CMC and silver nitrate was found to show gradual color expression from light yellow to dark brown and sol-gel transition over time. On the other hand, green-colored alginate sol without color change was induced by a simple reaction of alginate and silver nitrate. These results suggest that the polymer network structure of CMC reacts with silver nitrate to form an excellent colorimetric matrix with high selectivity.

The combination with silver ion precursors such as $AgNO_3$ resulted in facile and effective reduction of silver ions and formed metallogels containing AgNPs that experienced a sol-gel phase change. For gelation analysis, strain sweep test was performed with a constant 20.0 rad/s frequency at RT. Time and metal ion precursors were found to be critical factors in metallogel formation (Fig. 6a and b). Metallogels were prepared by adding a different amount of silver ion precursor ($AgNO_3$) at the same concentration to 1 mg/ml CMC. Although the gel strength is significantly different depending on the $AgNO_3$, in the presence of $AgNO_3$ the G' (storage modulus) of all samples is higher than G" (loss modulus) over the entire time of strains, which indicates the formation of metallogels [16].

The CMC solution, 0% (v/v) sample without *in-situ* synthesis of AgNPs, has an elastic

modulus of 0.29 ± 0.14 Pa as liquid-like in the measured strain range. In addition, it was confirmed that the gel strength increased with the increment of $AgNO_3$ ratio from 2.41 ± 0.27 Pa for 20% (v/v) to 19.47 ± 0.71 Pa for 30% (v/v) shown in Fig. 6a. The resulting strain sweep tests of 30% (v/v) gels at different times were shown Fig. 6b, which exhibit storage modulus indicating that the gel fabricates over gelation time at a constant angular frequency. These results are also consistent with the physical gelation that occurs between the functional groups of CMC and silver ions. These results suggest that silver ion precursors and time play a crucial role in the *in-situ* synthesis of AgNPs and the formation of metallogels. The storage modulus for the CMC-AgNPs gel (30 v/v%) was fonud to be greater than the loss modulus, which indicates that metallogels are finally formed (Fig. 6c). CMC-AgNPs metallogels are expected to be adopted in a commercial device in virtue of their elasticity, flexibility, and moldability.

To evaluate the selective colorimetric metallogel formation of CMC with each metal ions, several metal ion solutions such as copper (CuCl2), iron (FeCl3), gold (HAuCl4) and silver (AgNO3) ion precursors were added in an amount of 30% (v/v) into CMC solution (1 mg/ml). Samples were then observed for 14 days at RT (Fig. 6d). The reaction of CMC with noble metal ions such as Cu and Fe results in a metal substitution reaction, and then metal-coordinated nanocomposites are generated [23]. However, the metal exchange reaction does not occur with noble metal ions like gold, which is not chelated with the functional groups of the polymer [23]. The tilting method shows that gel behavior and colorimetric properties are not observed in all metals except silver. Under these concentrations, silver is a metal ion that

has a specific reaction to the CMC chain. When the silver ions contact CMC, the translucent gel, which was promptly organized, changed gradually to dark brown after 14 days. As a result, CMC-AgNPs metallogels are selectively prepared for silver ions, which the concentration of silver ion and time play an important role.
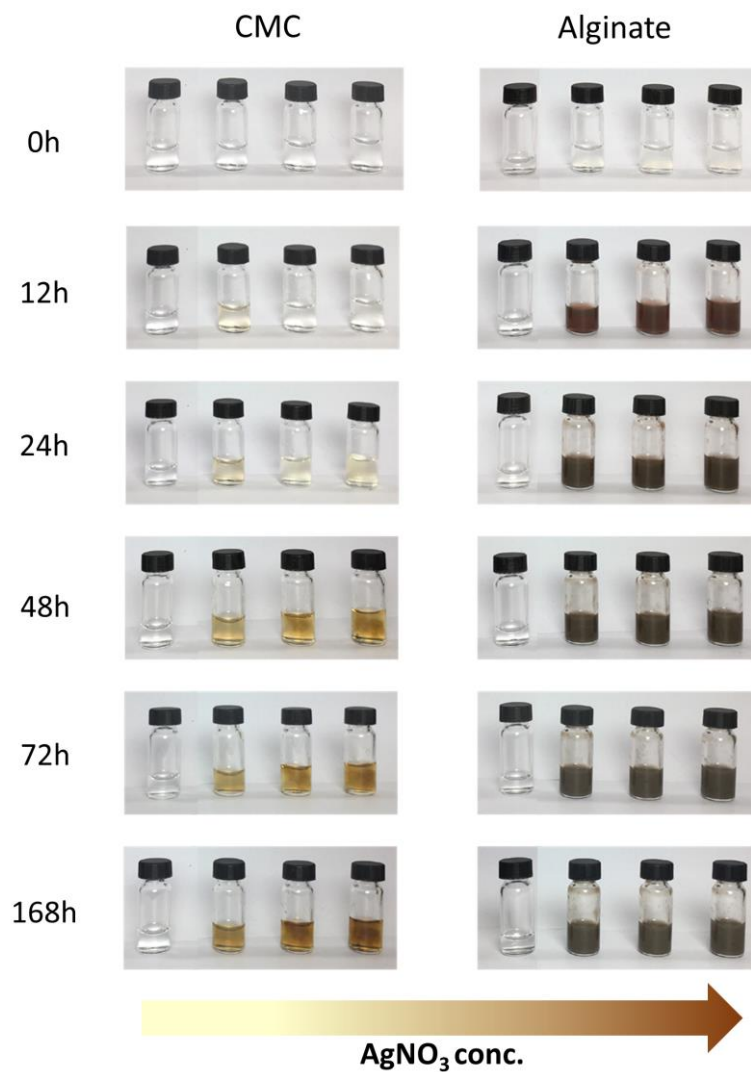
Figure 3. Visual inspection of reaction of biopolymer (carboxymethyl cellulose and alginate) and various concentrations of silver nitrate.
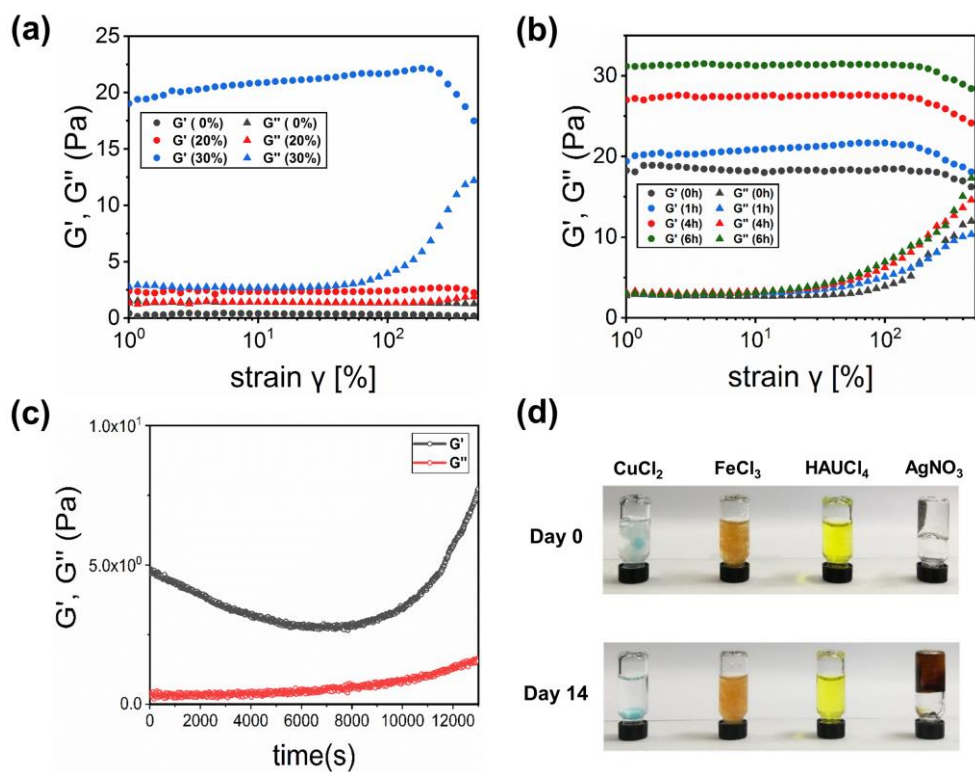
Figure 4. The rheological behavior of CMC-AgNPs metallogels. Strains sweeps of (a) gels with different concentrations of silver nitrate (b) gels which prepared at 30% (v/v) at different gelation times (c) dynamic time sweep performed on metallogels with 30% (v/v) AgNO$_3$ (d) Visual inspection of reaction of CMC with metal ion precursors.

Previous studies have proven that the carboxylic functional groups of CMC are highly capable of reducing and stabilizing metal nanoparticles [24]. Metal nanoparticles attached to the functional groups of the polymer chains are *in-situ* synthesized in the polymer network to function as the advantages of the two components of nanoparticle and hydrogel. That is, a biopolymer such as CMC, which has abundant carboxylic groups, act as efficient reductants for green synthesis of metal nanoparticles such as silver, gold, and copper nanoparticles [25, 26]. The presence of AgNPs in fabricated metallogels (30 v/v%) was demonstrated using UV-vis spectroscopy, FT-IR, and XRD (Fig. 7). The spectral data of CMC-AgNPs shown in Fig. 7a can help identify the functional groups of CMC involved in the synthesis of AgNPs. The intensity decrease of the band at 1586 cm^{-1} and 1411 cm^{-1}, corresponding to the vibrations of the COO − group asymmetric stretch and the COO – group symmetric stretch, respectively [27, 28]. The results indicated that nanoparticles are synthesized in metallogels obtained through the interaction between COO- groups and silver ion precursors.

The XRD patterns illustrated that the crystalline in nature of the CMC-AgNPs (Fig. 7b). The XRD peaks of metallogels with *in-situ* grown AgNPs are 2θ=38°, 44.4°, 65.2°, and 77.6°, which are consistent with (111), (200), (220) and (311) in the crystal plane according to the brag reflections; and it indexed as the face-centered cubic (fcc) structure of AgNPs [29]. The peak at 2θ=20° shown in pure CMC corresponds to the amorphous structure of CMC, and the peak shifted at 2θ=16.7° in CMC- AgNPs demonstrate that the polymer network structure was rearranged during silver ion binding [30]. AgNPs have a typical peak at about 410-430

nm due to unique localized surface plasmon resonance (LSPR) [16].

UV-vis absorption spectra of metallogel at 0 h, shown in Fig. 7c did not form peaks near 410nm consistent with white colored sol state of CMC-AgNPs. Meanwhile, the UV-vis peak amplitude at 410 nm was obtained at RT for 7 days (Fig. 7d). The obtained graph has a linear correlation, and it can be confirmed that the LSPR characteristic of the nanoparticles is prominent. The formation of CMC-AgNPs metallogel involved the conversion to the polymer matrix of the CMC solution by *in-situ* nanoparticle synthesis following the complexation of the metal cation with the carboxylate group on CMC.
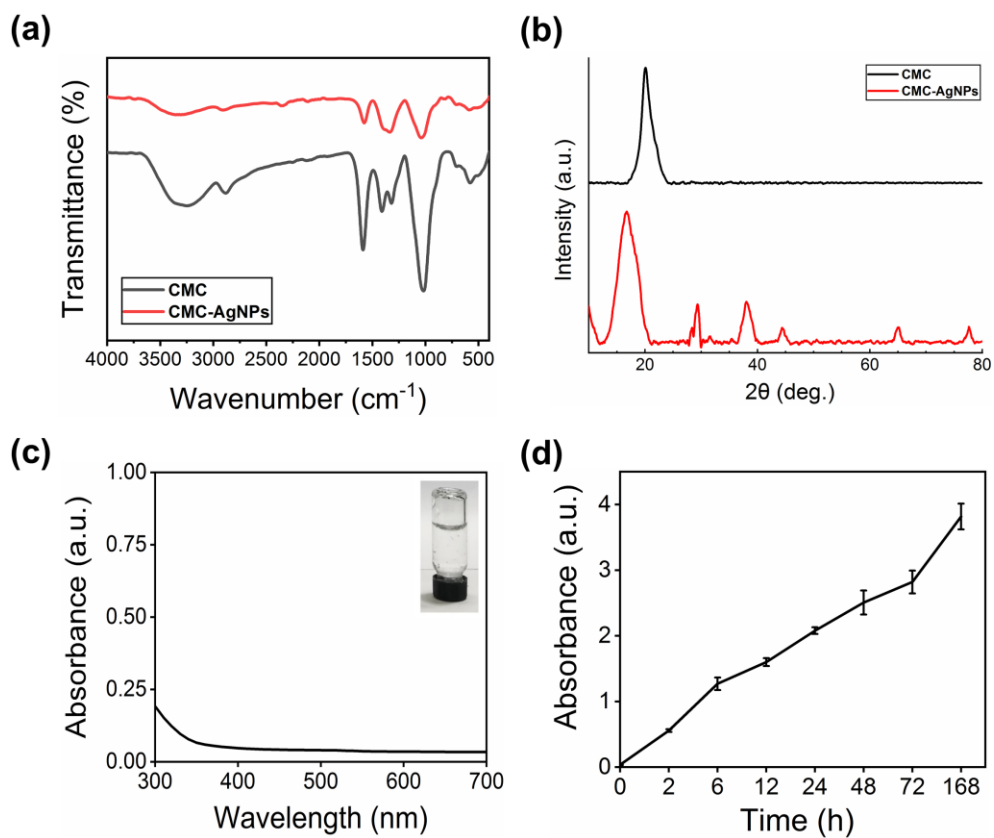
Figure 5. (a) FT-IR spectra (b) XRD patterns (c) UV-vis absorption spectrum as-synthesized

CMC-AgNPs (d) peak amplitude at 410 nm.

3.2. The colorimetric transition of silver nanoparticles depending on time and temperature

Metallogels undergo colorimetric change deserved by the specific optical properties of *in-situ* synthesized AgNPs. TEM and UV-vis data were analyzed to determine the growth conditions of the AgNPs after storing the metallogel at each temperature (4 ℃, RT (= 25 ℃), 60 ℃). The typical HR-TEM micrograph, which presented the morphology, size distributions, and aggregation of AgNPs, are shown in Fig. 8a and c. As can be seen in the photograph, the particle size of the nanoparticles formed at 60 ℃ is much larger than AgNPs produced at RT. Since the only difference in the manufacturing process is only the temperature, it can be seen that temperature is a vital factor for the growth of AgNPs. After 14 days, the size distribution of the nanoparticles *in-situ* synthesized at RT was 19.84 ±14.99 nm and had a uniform spherical shape.; Besides, evidence that the nanoparticles are well dispersed in the metallogels can be seen as the individual particles are separated (Fig. 8a and b). On the other hand, the size of AgNPs prepared at 60 ℃ was proven to grow compared to RT (Fig. 8c). This result shows the coexistence of nanoparticles of 80-120 nm and small nanoparticles, suggesting that high temperature quickly leads to the growth of AgNPs within metallogels. At high temperatures, silver ions are promoted to silver atom reduction, and some of the smaller AgNPs generated at the initial stage adhere to existing particles, leading to the synthesis of large AgNPs [31]. That is, as the nanoparticles are synthesized at higher temperatures in the polymer matrix, larger

28

nanoparticles are formed.

The EDS analysis of AgNPs also confirmed the presence of silver elemental composition (Fig. 9a and b) [22]. It was confirmed that the silver element was formed in the metallogel through the clear peak at 3 keV, which is signals of surface plasmon resonance of silver. The other signal like copper, also has been observed due to the use of a TEM grid.
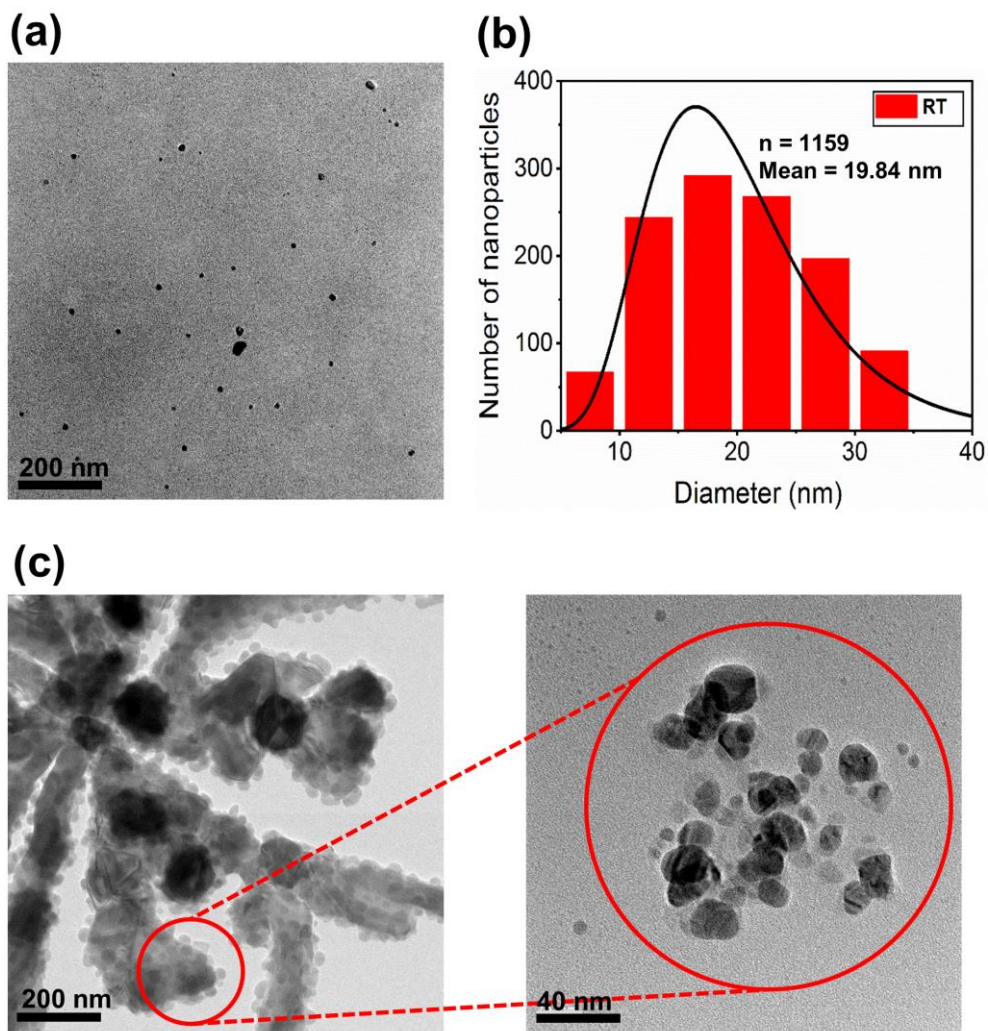
Figure 6. HR-TEM image of silver nanoparticles after 14 days (a) at RT (d) at 60 ℃. (b) size

distribution of AgNPs at RT.

(a)

Element	Weight%	Atomic%
Cu K	69.38	79.37
Ag L	30.62	20.63
Totals	100.00	

Full Scale 705 cts Cursor: 0.000 keV

(b)

Element	Weight%	Atomic%
Cu K	30.82	43.06
Ag L	69.18	56.94
Totals	100.00	

Full Scale 1290 cts Cursor: 0.000 keV
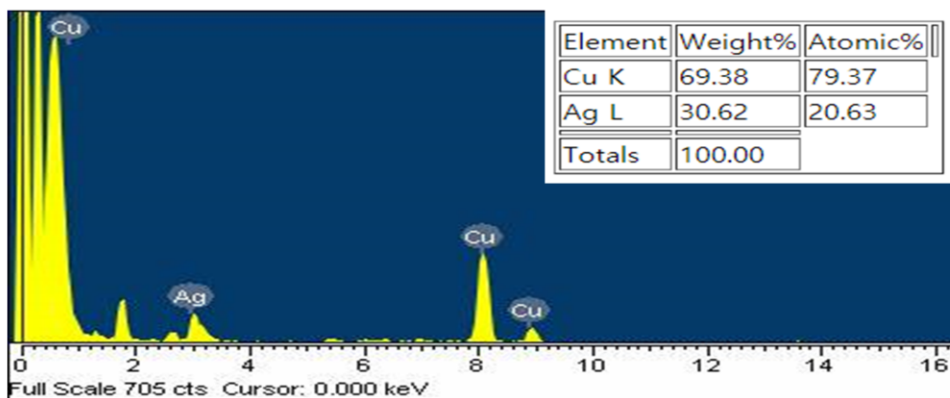
Figure 7. EDS analysis of AgNPs synthesized (c) at RT (e) at 60 °C.

31

Metal nanoparticles exhibit specific optical properties by interacting with particular wavelengths of light. The absorbance of AgNPs dispersed in the metal gel over time was determined to confirm the absorption wavelength of substances within metallogels using a UV-vis spectrometer (Fig. 10). The metallogels (30 v/v%) used in the analysis were placed at 4 °C and RT, respectively. The absorbance of metallogels stored at 4 °C remained unchanged with low absorbance values during the experiment (Fig. 10a). When the metallogels were maintained at RT, the absorption spectrum has the highest peak of 400-500nm and the time-dependent increase in absorbance shown in Fig. 10b. The UV-vis spectrum of me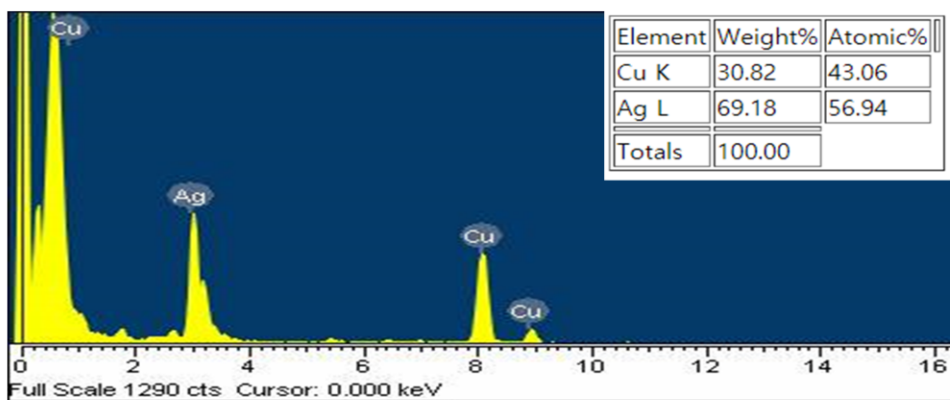tallogel at 4 °C shows the nonexistence of AgNPs because no characteristic peaks are formed. The particles prepared at RT exhibited an extremely acute peak at 440 nm from 12 hours to 168 hours, which is ascribed to the characteristic surface plasmon resonance band of the AgNPs. Although the two metallogls were kept under the same conditions except for the temperature, the reduction of Ag ions in RT gels was faster. At the same time, the absorbance values at RT increase, indicating that silver ions are easily reduced to silver atoms and the color of the metallogels changes from light yellow to dark brown. Moreover, the absorption band was slightly red-shifted over several days. This is because, as AgNP fused with adjacent particles, the localized surface plasmon shifted to the right. A high absorption rate of light over time means that the color of the nanoparticles becomes thicker over time, which absorbs more light in the same wavelength band [32]. These results suggest that low temperature interferes with the growth as well as the nucleation of AgNPs. The elongated heating resulted in a significant
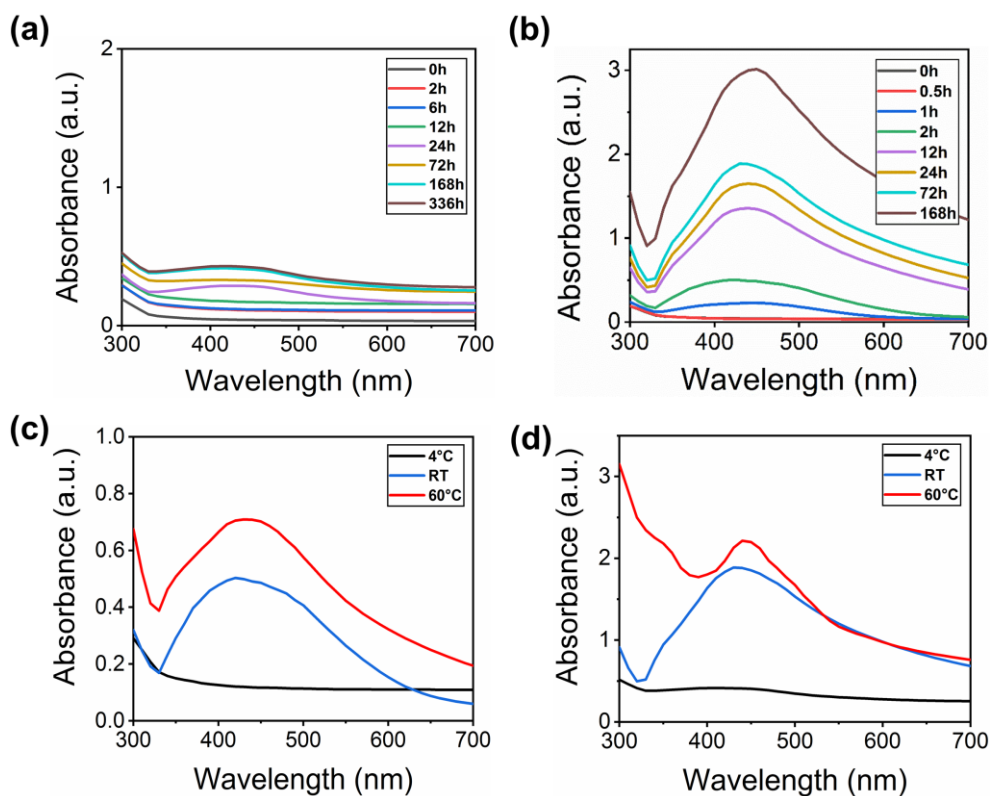
32

peak with increasing the absorbance.

Figure 8. UV-vis absorption spectra of CMC-AgNPs metallogel prepared (a) at 4 ℃ (b) at RT

for different period (c) after 2 h (b) after 72 h for different temperatures.

The UV-vis spectra of the metallogels prepared at 4 ℃, RT, and 60 ℃ were also confirmed. After 2 hours, the LSPR peak of AgNPs red shifted approximately from 420nm to 430nm by increasing the storage temperature (Fig. 10c). Increase in absorbance of all samples after 72 hours observed with a distinct intensity from RT to 60 ℃ (Fig. 10d). Experiment results indicate that the number and size of newly synthesized AgNPs are increased depending on temperature and time. Thus, temperature and time are critical parameters affecting the synthesis and growth of nanoparticles consistent with the results of the TEM image, causing color development due to the visually identifiable LSPR red shift of AgNPs from yellow to brown. It provides the ability to predict the thermal history of the product.

3.3 Evaluation of color expression of CMC-AgNPs metallogels as a colorimetric sensor

The results presented in Fig. 11a are color response charts of CMC-AgNPs metallogel for different reaction time and temperature. Metallogels were generated by mixing 1 mg/ml CMC solution with 0.1 M $AgNO_3$ (30 v/v%). Experiments were carried out at 4 ℃, RT, and 60 ℃ with reaction times of 1-336 hours. Following the previous results, the visual color of metallogels was changed from light yellow to brown depending on the time, temperature, and concentration of silver ion precursors. As the small amount of silver precursors solution was

added into CMC, the intensity of the color becomes stronger due to the interaction of the functional group of the polymer with a larger number of silver ions, so that it can be observed with the naked eye. Besides, it was confirmed that as the reaction time was extended, a color transition occurs due to the formation and growth of AgNPs. At the same concentration and time, the higher the temperature from 4 ℃ to 60 ℃, the faster the colorimetric change is detected. A colorimeter was utilized to quantify the exact total color difference of metallogels with the most noticeable color change. The total color difference at a different storage temperature of CMC-AgNPs metallogel (30% v/v) is shown in Fig. 11b, which was calculated by measuring L *, a * and b * values. Herein, the total color difference is the gap between the sample immediately after fabrication (0h) without AgNPs and the metallogel measured at each time (2, 4, 6, 12, 24, 48, 72h). When metallogel is placed at 60 ℃, the TCD value increases rapidly up until 12 hours and then decreases. The TCD of the sample stored at RT slowly grows, but it promptly has risen from 12 hours to the maximum value. On the other hand, the TCD of a sample at refrigerated storage temperature (4 ℃) gradually increases without noticeable change until 24 hours indicating that the growth of nanoparticles is inhibited when compared to different temperatures.
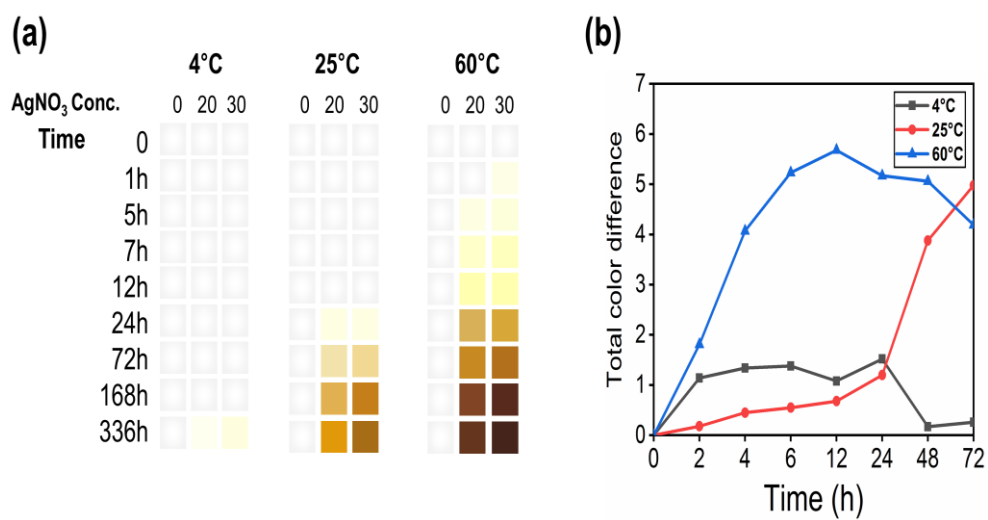
Figure 9. (a) The color chart (b) Total color difference of CMC-AgNPs metallogels at 4 ℃, 25 ℃, 60 ℃ for different time.
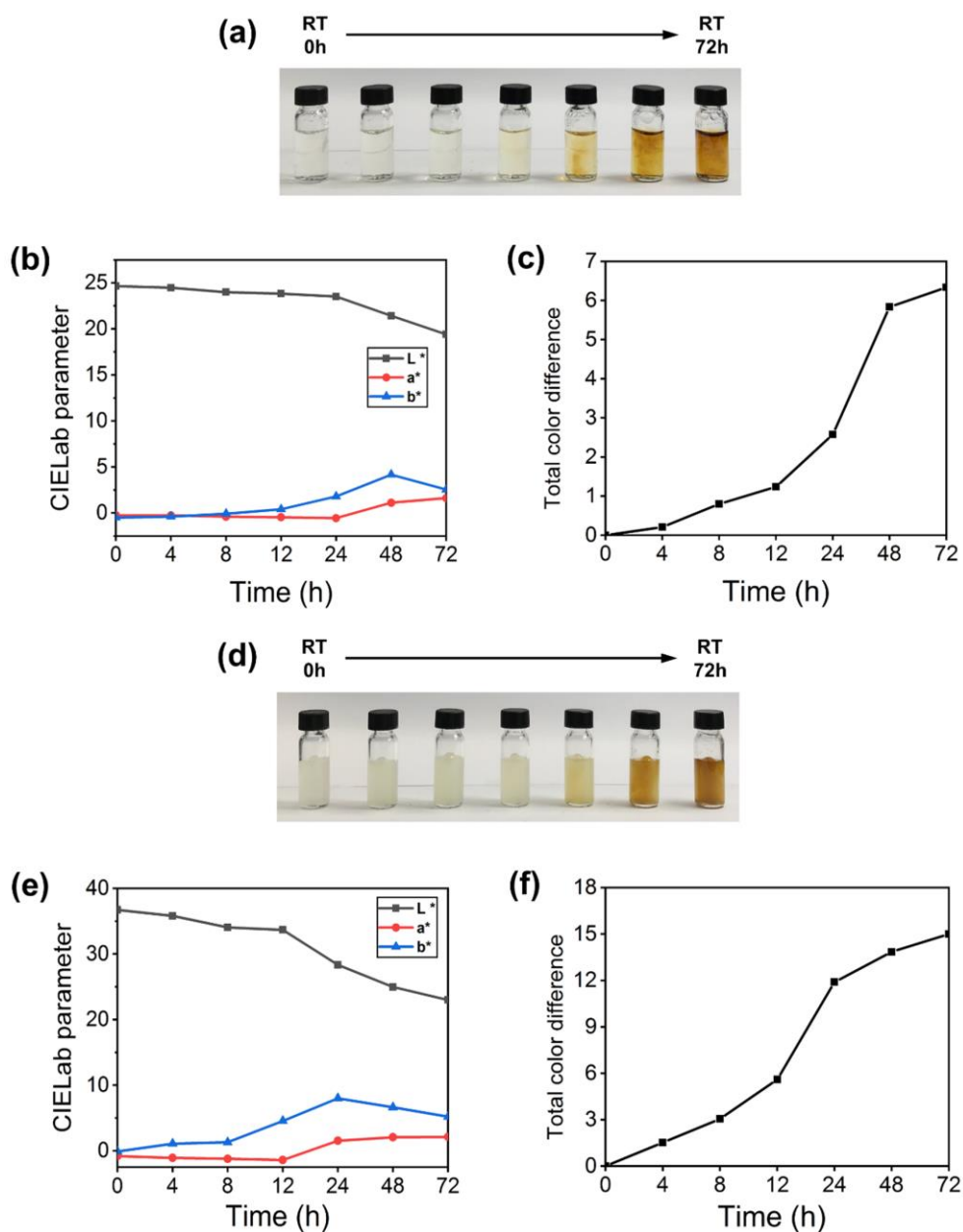
Figure 10. (a, d) Color evolution (b, e) L, a, b CIELAB parameter (c, f) Total color difference

of CMC-AgNPs metallogel which first located at 4 ℃, -20 ℃ for 2h, after exposure to RT for

different time then placed 4 ℃, -20 ℃ for further 24 h, respectively.

In general, perishable products intended for metallogel applications are mostly stored at low temperature and should be maintained at low temperatures all the time [33]. For example, most vaccines should be kept at 2-8 ℃ [34]. However, the plot to be exposed to RT or high temperature is very natural during distribution, storage and sale. Color transitions should not only change intensively as the temperature abuse time persists but should also be irreversible, even if they are frozen later again. I exposed the metallogel, which was stored frozen for 2 hours at 4 ℃ and -20 ℃, to the temperature abuse condition (RT) for each time (0, 4, 8, 12, 24, 48, 72h) and then returned the sample to freezing (4 ℃, -20 ℃) for 72 hours.

When the metallogel stored at 4 ℃ was exposed to temperature abuse conditions; the color became darker when compared to the control (sample with RT exposure of 0 h) as the temperature abuse period increased (Fig. 12a). These results correspond to the total color difference (TCD) as well as the L *, a *, b * values in CIELab shown in Fig. 12b and c. Samples placed at -20 ℃ also have a dark brown metallogel that experiences temperature abuse and TCD values also increase with RT exposure (Fig. 12d and f). As the L* value decreases, with increased a* and b* values, the color of metallogel becomes darker from yellow to brown (Fig. 12e). The TCD value likewise increases proportionally as the RT

exposure duration is extended. What is notable is that the metallogel, which has undergone temperature abuse, does not come back again even though it moves to the appropriate storage temperature (4 ℃, -20 ℃). Our current platform satisfies Irreversible color change, which is the fundamental requirement of TTI applied to low-temperature distribution products. Depending on the size of the sensor, a minimum of 1-1.3 ml of metallogel is produced with low cost, which is suitable for use as a disposable sensor.

Chapter 4. Conclusions

In summary, a novel colorimetric sensor has been developed that incorporates CMC-AgNPs metallogel exploiting the LSPR characteristics of AgNPs. The sensing platform is based on metallogels fabricated within a few minutes under specific conditions such as the amount of metal ion precursors and time, which can be detected quickly, intuitively and directly, judged by the growth of *in-situ* synthesized AgNPs in metallogels. Green synthesis of AgNPs with biopolymer introduces a cost-efficient and eco-friendly sensing platform. When the metallogel is exposed to abused temperature, the visual color becomes more distinct from light yellow to dark brown. The irreversible color change can be observed with the naked eye. The system is versatile as an indicator to identify of when products are no longer safe based on time-temperature exposure history as well as to assure the quality of frozen stored products such as foods, medicines, chemicals during the distribution. Additionally, it is a precise, rapid, eco-friendly, low-cost sensing system suitable for industrial application.

References

1. Lahiri, D.K. and B. Schnabel, *DNA isolation by a rapid method from human blood samples: effects of MgCl2, EDTA, storage time, and temperature on DNA yield and quality.* Biochem Genet, 1993. **31**(7-8): p. 321-8.

2. Bell, K.N., et al., *Risk factors for improper vaccine storage and handling in private provider offices.* Pediatrics, 2001. **107**(6): p. E100.

3. Devlieghere, F., L. Vermeiren, and J. Debevere, *New preservation technologies: Possibilities and limitations.* International Dairy Journal, 2004. **14**(4): p. 273-285.

4. Aung, M.M. and Y.S. Chang, *Temperature management for the quality assurance of a perishable food supply chain.* Food Control, 2014. **40**: p. 198-207.

5. Centers for Disease Control and Prevention (CDC), 2010

6. Wang, Y.C., L. Lu, and S. Gunasekaran, *Biopolymer/gold nanoparticles composite plasmonic thermal history indicator to monitor quality and safety of perishable bioproducts.* Biosens Bioelectron, 2017. **92**: p. 109-116.

7. Wang, S.D., et al., *Review of Time Temperature Indicators as Quality Monitors in Food Packaging.* Packaging Technology and Science, 2015. **28**(10): p. 839-867.

8. Masoud Ghaani, et al., An overview of the intelligent packaging technologies in the food sector. Trends in Food Science & Technology, 2016. 51: p. 1-11.

9.   Tao, H., et al., *Silk-Based Conformal, Adhesive, Edible Food Sensors.* Advanced Materials, 2012. **24**(8): p. 1067-1072.

10.   Bobelyn, E., M.L.A.T.M. Hertog, and B.M. Nicolai, *Applicability of an enzymatic time temperature integrator as a quality indicator for mushrooms in the distribution chain.* Postharvest Biology and Technology, 2006. **42**(1): p. 104-114.

11.   Wanihsuksombat, C., V. Hongtrakul, and P. Suppakul, *Development and characterization of a prototype of a lactic acid-based time-temperature indicator for monitoring food product quality.* Journal of Food Engineering, 2010. **100**(3): p. 427-434.

12.   Kim, J.U., et al., *Kinetic modeling and characterization of a diffusion-based time temperature indicator (TTI) for monitoring microbial quality of non pasteurized angelica juice.* Lwt-Food Science and Technology, 2016. **67**: p. 143-150.

13.   Zhang, C., et al., *Time--temperature indicator for perishable products based on kinetically programmable Ag overgrowth on Au nanorods.* ACS Nano, 2013. **7**(5): p. 4561-8.

14.   Kuhn, S., et al., *Enhancement of single-molecule fluorescence using a gold nanoparticle as an optical nanoantenna.* Physical Review Letters, 2006. **97**(1).

15.   Odegard, G.M., T.C. Clancy, and T.S. Gates, *Modeling of the mechanical properties of nanoparticle/polymer composites.* Polymer, 2005. **46**(2): p. 553-562.

16.   Mornet, S., et al., *Magnetic nanoparticle design for medical diagnosis and therapy.*

Journal of Materials Chemistry, 2004. **14**(14): p. 2161-2175.

17. Shi, G.X., et al., *A novel electrically conductive and biodegradable composite made of polypyrrole nanoparticles and polylactide.* Biomaterials, 2004. **25**(13): p. 2477-2488.

18. Timothy V.Duncan, Applications of nanotechnology in food packaging and food safety: Barrier materials, antimicrobials and sensors, Journal of Colloid and Interface Science, 2011, 363(1): p. 1-24.

19. Piepenbrock, M.O.M., N. Clarke, and J.W. Steed, *Rheology and silver nanoparticle templating in a bis(urea) silver metallogel.* Soft Matter, 2011. **7**(6): p. 2412-2418.

20. Lin, Q., et al., *A novel imidazophenazine-based metallogel act as reversible H2PO4-sensor and rewritable fluorescent display material.* Sensors and Actuators B-Chemical, 2017. **251**: p. 250-255.

21. Pablos, J.L., et al., *Solid polymer and metallogel networks based on a fluorene derivative as fluorescent and colourimetric chemosensors for Hg(II).* Reactive & Functional Polymers, 2014. **79**: p. 14-23.

22. Chang, C.Y., et al., *Superabsorbent hydrogels based on cellulose for smart swelling and controllable delivery.* European Polymer Journal, 2010. **46**(1): p. 92-100.

23. Amendola, V., O.M. Bakr, and F. Stellacci, *A Study of the Surface Plasmon Resonance of Silver Nanoparticles by the Discrete Dipole Approximation Method: Effect of Shape, Size, Structure, and Assembly.* Plasmonics, 2010. **5**(1): p. 85-97.

24. Liu, G.H. and J.Y. Yang, *Content-based image retrieval using color difference histogram.* Pattern Recognition, 2013. **46**(1): p. 188-198.

25. Solomon, M.M., H. Gerengi, and S.A. Umoren, *Carboxymethyl Cellulose/Silver Nanoparticles Composite: Synthesis, Characterization and Application as a Benign Corrosion Inhibitor for St37 Steel in 15% H2SO4 Medium.* Acs Applied Materials & Interfaces, 2017. **9**(7): p. 6376-6389.

26. Nadagouda, M.N. and R.S. Varma, *Synthesis of thermally stable carboxymethyl cellulose/metal biodegradable nanocomposites for potential biological applications.* Biomacromolecules, 2007. **8**(9): p. 2762-7.

27. He, F., D.Y. Zhao, and C. Paul, *Field assessment of carboxymethyl cellulose stabilized iron nanoparticles for in situ destruction of chlorinated solvents in source zones.* Water Research, 2010. **44**(7): p. 2360-2370.

28. Hebeish, A.A., et al., *Carboxymethyl cellulose for green synthesis and stabilization of silver nanoparticles.* Carbohydrate Polymers, 2010. **82**(3): p. 933-941.

29. Chen, J., et al., *Microwave-assisted green synthesis of silver nanoparticles by carboxymethyl cellulose sodium and silver nitrate.* Materials Chemistry and Physics, 2008. **108**(2-3): p. 421-424.

30. Bozaci, E., et al., *Application of carboxymethylcellulose hydrogel based silver nanocomposites on cotton fabrics for antibacterial property.* Carbohydrate Polymers, 2015. **134**: p. 128-135.

31.   Cuba-Chiem, L.T., et al., *In situ particle film ATR FTIR spectroscopy of carboxymethyl cellulose adsorption on talc: Binding mechanism, pH effects, and adsorption kinetics.* Langmuir, 2008. **24**(15): p. 8036-8044.

32.   Balaji, D.S., et al., *Extracellular biosynthesis of functionalized silver nanoparticles by strains of Cladosporium cladosporioides fungus.* Colloids and Surfaces B-Biointerfaces, 2009. **68**(1): p. 88-92.

33.   Yang, F., et al., *Synthesis, characterization, and applied properties of carboxymethyl cellulose and polyacrylamide graft copolymer.* Carbohydrate Polymers, 2009. **78**(1): p. 95-99.

34.   Pastoriza-Santos, I. and L.M. Liz-Marzan, *Reduction of silver nanoparticles in DMF. Formation of monolayers and stable colloids.* Pure and Applied Chemistry, 2000. **72**(1-2): p. 83-90.

35.   Su, K.H., et al., *Interparticle coupling effects on plasmon resonances of nanogold particles.* Nano Letters, 2003. **3**(8): p. 1087-1090.

36.   Guilbert, S., N. Gontard, and L.G.M. Gorris, *Prolongation of the shelf-life of perishable food products using biodegradable films and coatings.* Food Science and Technology-Lebensmittel-Wissenschaft & Technologie, 1996. **29**(1-2): p. 10-17.

37.   Matthias, D.M., et al., *Freezing temperatures in the vaccine cold chain: a systematic literature review.* Vaccine, 2007. **25**(20): p. 3980-6.

국문초록

비색계 센서로서 은 나노입자의 *in-situ* 합성으로 유도된 카르복시메틸 셀룰로오스 금속겔에 관한 연구

송유진

나노융합전공

융합과학부

서울대학교 융합과학기술대학원

최근 온도 상승, 안정성이 보증되지 않은 콜드 체인, 그리고 유통 과정 중 보관 상태 불량 등으로 인하여 저온 유통 제품의 안전에 대한 사회적 관심과 우려가 높아지고 있다. 저온 유통 제품의 저장 및 유통과정에서 내외부적인 다양한 요인에 의하여 복합적인 품질 변화가 수반되는데, 특히 품질 변화에서 가장 중요

한 요소는 주로 환경요인인 온도에 직접적인 영향을 받는다. 이에 소비자가 제품의 신선도를 판별하는 것을 돕기 위한 확산, 효소 및 광 변색성에 기초한 다양한 온도 모니터링 기술이 연구되고 있지만, 종래 기술은 실험방법이 복잡하고 값이 비싸 소비자가 식품을 구매하는 과정에서 이용되지 못한다. 본 연구에서는 시간과 온도에 따라 은 나노입자의 크기 및 색이 변화하는 원리에 의거하여 저온유통식품의 품질 상태를 알아보는 모니터링 센서 장치를 개발하였다. Carboxymethyl cellulose(CMC)와 같은 천연고분자 및 나노입자를 이용하여 저온에서 보관하는 부패하기 쉬운 제품의 온도 이력 및 품질을 모니터링하기 위해 CMC-AgNPs 금속겔을 기반으로 하는 새로운 비색계 센싱 플랫폼이 제안되었다. Ag+ 이온의 존재 하에서 제조된 CMC 금속겔은 생체 고분자의 이온 가교 결합과 반응물 사이의 복합체 형성, 그리고 온도와 시간에 의존하여 무색에서 암갈색으로 금속겔의 색을 이끌도록 고안된 은 나노입자의 in-situ 합성을 통합한다. 생성된 금속겔과 은 나노입자는 유변학, XRD 및 FT-IR에 의해 관찰되었다. 또한 온도, 시간 및 금속 이온 전구체의 농도에 따른 색 변화는 자외선 가시 분광법(UV-vis)과 비색법으로 조사하였다.

CMC-AgNPs 금속겔은 AgNO3의 비율이 30% (v/v) 일 때, 탄성 계수가 19.47 ± 0.71 Pa로 탄성 계수가 0.29 ± 0.14 Pa인 CMC 용액과 비교하여 약 67.1배 증가하여 겔이 유의미하게 생성되었다. 또한 CMC는 은 이온 전구체에 대하여 선택적으로 비색계 특성을 지닌 금속 겔을 형성하였다. FT-IR 스펙트럼을 통해 금속 겔 형성에 관여하는 CMC의 작용기를 입증하였으며, XRD 피크는 은 나노입자의 결

정 구조와 일치하였다. UV-vis 흡수 스펙트럼을 통해 얻은 410nm 피크는 금속 겔 내부에 형성된 은 나노입자의 LSPR 특성과 상응하였다. 금속겔에 in-situ로 합성된 은 나노입자의 구조 및 크기는 온도에 따라 HR-TEM 현미경으로 관찰되었다. 실내 온도 (25 ℃)에서 합성된 은 나노입자의 크기 분포는 19.84 ± 14.99 nm이며 균일하게 분산된 구형의 형태를 가지는 반면, 고온 (60 ℃)에서 생성된 은 나노입자는 나노입자가 공존하여 80-120 nm의 크기를 가졌다. 금속겔 내에서 합성된 은 나노입자는 시간과 온도에 의존적으로 옅은 노란색에서 황색, 그리고 짙은 갈색까지의 눈으로 감지할 수 있는 색의 변화를 나타낸다. 실내 온도 (25 ℃) 또는 고온 (60 ℃)과 같은 적절하지 않은 보관 온도에 대한 노출 시간이 길어질 수록, 금속 겔의 색상은 더욱 진해졌으며, 이는 L*, a*, b* 값을 통해 얻어진 total color difference (TCD)값의 증가를 통하여 확인할 수 있었다.

CMC-AgNPs 금속겔 기반의 센싱 플랫폼은 구조가 단순하고 전원 등의 외부 구조를 필요로 하지 않아 저비용으로 제작이 가능하며 소형화가 용이하여 휴대용으로 제작하거나 유통식품에 탈 부착하는 형태로 제작이 가능하다. 특히 은 나노입자의 생성 비율과 응집상태를 적절히 조절하여, 다양한 저장 및 유통 온도를 거치는 다양한 제품군에 활용될 수 있다. 또한 복잡한 사용법을 숙지할 필요 없이 물리적인 동작만으로 쉽게 활성화 할 수 있고 육안으로 관측되는 색상만으로 식품의 변질 유무 파악이 가능하므로 직관적이라는 장점이 있다. 환원제나 안정제로서 화학물질이 첨가되지 않아 독성이 없으며, TTI가 파손되어 구성 물질이 누출되었을 경우에도 인체에 비교적 해롭지 않은 물질만으로 구성되어 있어

비교적 환경 친화적이다. 해당 TTI 센서는 비용 절감, 휴대성 및 단순성의 특징을 가지므로 저온유통식품의 안전한 유통관리 정착, 폐기물 감소 및 식중독의 사전 예방 등의 사회적 비용을 감소시킬 수 있는 이점을 가질 것이며, 나노기술과 TTI 기술의 접목은 향후 TTI 산업 성장의 새로운 패러다임을 마련할 수 있을 것이다.